Electronic, dynamical, and thermal properties of ultra-incompressible superhard rhenium diboride: A combined first-principles and neutron scattering study

W. Zhou,[1,2,*] H. Wu,[1,3] and T. Yildirim[1,2]
[1]*NIST Center for Neutron Research, National Institute of Standards and Technology, Gaithersburg, Maryland 20899, USA*
[2]*Department of Materials Science and Engineering, University of Pennsylvania, Philadelphia, Pennsylvania 19104, USA*
[3]*Department of Materials Science and Engineering, University of Maryland, College Park, Maryland 20742, USA*
(Received 27 August 2007; published 19 November 2007)

Rhenium diboride is a recently recognized ultra-incompressible superhard material. Here we report the electronic (e), phonon (p), e-p coupling, and thermal properties of ReB_2 from first-principles density-functional theory calculations and neutron scattering measurements. Our calculated elastic constants (c_{11} =641 GPa, c_{12}=159 GPa, c_{13}=128 GPa, c_{33}=1037 GPa, and c_{44}=271 GPa), bulk modulus ($B \approx 350$ GPa) and hardness ($H \approx 46$ GPa) are in good agreement with the reported experimental data. The calculated phonon density of states agrees very well with our neutron vibrational spectroscopy result. Electronic and phonon analysis indicates that the strong covalent B-B and Re-B bonding is the main reason for the super incompressibility and hardness of ReB_2. The thermal expansion coefficients, calculated within the quasiharmonic approximation and measured by neutron powder diffraction, are found to be nearly isotropic in a and c directions and only slightly larger than that of diamond in terms of magnitude. The excellent agreement found between calculations and experimental measurements indicate that first-principles calculations capture the main interactions in this class of superhard materials, and thus can be used to search, predict, and design new materials with desired properties.

DOI: 10.1103/PhysRevB.76.184113 PACS number(s): 71.20.−b, 62.20.Dc, 63.20.−e, 65.40.−b

I. INTRODUCTION

Hard materials are of great scientific interest due to their numerous technological applications. Unfortunately, almost all superhard materials (diamond, cubic BN, etc.) are expensive because they either occur naturally in limited supplies or have to be made at high pressure synthetically. Therefore, intense research efforts have been carried out to design superhard materials.[1] Recently, it was found that rhenium diboride can be synthesized at ambient pressure with potentially low cost, and the resulting ReB_2 crystal has superincompressibility along the c axis, comparable to that of diamond, and high hardness, comparable to that of cubic BN.[2] The mechanical properties of ReB_2 were also correctly predicted by a recent theoretical work.[3] To more fully understand this unusual material, we have used a combined first-principles and neutron scattering study to further investigate the electronic, elastic, phonon, and thermal properties of ReB_2.

II. METHODS AND MATERIALS

Our calculations were performed within the plane-wave implementation of the generalized gradient approximation (GGA) to density-functional theory (DFT) in the PWSCF package.[4] We used Vanderbilt-type ultrasoft potential with Perdew-Burke-Ernzerhof exchange correlation. A cutoff energy of 680 eV and a $16\times16\times6$ k-point mesh (generated using the Monkhosrt-Pack scheme) were found to be enough for total energy to converge within 0.01 meV/atom. Spin-polarized calculations resulted in zero spontaneous spin polarization for the material investigated; thus here we focus on the results from spin-restricted calculations.

Neutron scattering measurements were undertaken at the NIST Center for Neutron Research. The inelastic neutron scattering (INS) measurements were performed with the BT-4 filter-analyzer neutron spectrometer. The neutron powder diffraction was performed with the BT-1 high-resolution powder diffractometer. ReB_2 powder sample used in both experiments was synthesized using the method of direct heating of the elements (Re and ^{11}B) in vacuum at 1273 K, as reported in Ref. 2. The purpose of using ^{11}B isotope is to avoid the large neutron absorption of normal boron.[5]

III. RESULTS AND DISCUSSION

ReB_2 has a simple hexagonal structure (space group $P6_3/mmc$) with experimental a=2.900 Å and c=7.478 Å, as shown in Fig. 1(a).[6] The two Re atoms occupy the sites (1/3,2/3,1/4) and (2/3,1/3,3/4) while the four boron atoms occupy the sites (2/3,1/3,z), (1/3,2/3,1/2+z), (2/3,1/3,1/2−z), (1/3,2/3,1−z) with experimental z =0.048. We first optimized both the lattice parameters and the atomic positions of the ReB_2 structure. The relaxed parameters (without considering the zero point motion), a =2.9007 Å, c=7.4777 Å, and z=0.0478, all agree very well with the experimental values. We note that the crystal structure of ReB_2 is quite different from other metal diboride compounds, a majority of which assume MgB_2 type structure. In MgB_2, boron atoms are on the same plane, with a graphene structure[7,8] while they are buckled in ReB_2. In addition, Mg is located above the center of B hexagon in MgB_2, while in ReB_2, Re is located right on top of the B atom. The structural configuration of ReB_2 is mainly due to the strong hybridization of Re-d and B-p orbitals, which we will discuss in detail below.

To understand the high hardness of ReB_2, it is essential to look at its electronic structure. According to the calculated

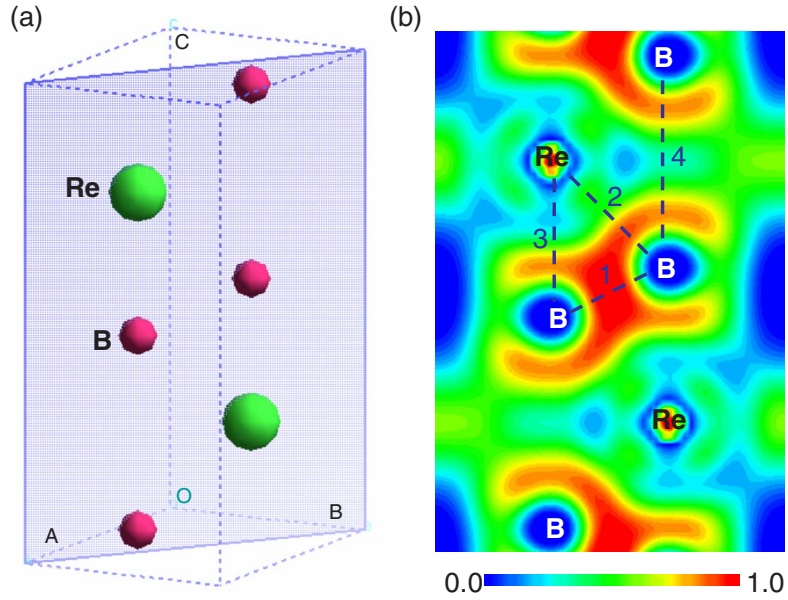

FIG. 1. (Color online) (a) A unit cell of ReB_2. (b) The electron localization function of the (1 1 −2 0) crystal plane. The four types of chemical bonds are denoted using dashed lines. The strong directional, covalent B-B (labeled "1") and Re-B (labeled "2" and "3") bonding are apparent.

valence charge distribution, there exist large electron densities between two neighboring B atoms, and between the Re atoms and its neighboring B atoms, indicating strong directional, covalent B-B and Re-B bonding. This is as expected, since a material with large hardness must contain highly directional, short and strong bonds.[9,1,2] To get more detailed information about the bonding nature, we performed electron localization function (ELF) analysis[10] and Mulliken bond population analysis.[11] In particular, the ELF plot is very useful in terms of distinguishing different bonding interactions. The value of ELF is in the range of 0 to 1 by definition. High ELF value corresponds to a low Pauli kinetic energy, as can be found in covalent bond. A value of ELF near 0.5 corresponds to delocalized electron density as found in metallic bonding. The ELF plot of the (1 1 −2 0) crystal plane of ReB_2 is shown in Fig. 1(b). The dominant feature is the rather strong B-B bond (labeled "1"). The two Re-B bonds (labeled "2" and "3") clearly have different bonding characters. The B-B bond along the c axis (labeled "4") has a large length, but ELF shows that its contribution to the overall bonding is not negligible. More quantitative bond population analysis (see Table I) confirms that the B-B bonding is very strong and highly covalent, with essentially a double bond nature. Interestingly, the Re and its two neighbored B atoms sitting right above and below it (along the c axis) form antibonding, while Re forms strong covalent bonding with all other six B neighbors. In Table I, the real-space force constants between these ions, obtained from the phonon calculation (discussed later), are also shown, which indicate strong B-B and Re-B bonding as well. The B-B and Re-B bonds, all together, form a covalently bonded three-dimensional network.

TABLE I. The calculated bond population, bond length, and real-space force constants for selected pairs of ions in a (1,1,−2,0) plane in ReB_2. The positive (negative) bond population indicates bonding (antibonding) character. Note that the force constants are very large for nearest neighbor B-B and Re-B pairs, indicating very strong local covalent bonding.

No.	Bond	Population	Length (Å)	Force constant (eV/Å^2)
1	B-B	1.96	1.820	4.55
2	Re-B	0.72	2.257	4.34
3	Re-B	−0.25	2.227	5.08
4	B-B	−0.14	3.025	1.36

In Fig. 2(a), we show the electronic band structure of ReB_2. The total density of states (DOS) and the partial DOS projected onto atomic orbitals are shown in Fig. 2(b). Clearly, the material is metallic and the electronic structure of ReB_2 near the Fermi level is governed by a strong hybridization of Re-d and B-p orbitals, which results in the strong covalent bonding of B-B and Re-B. In terms of this bonding characteristic, ReB_2 is similar to the previously well studied OsB_2,[12–15] although the latter has an orthorhombic structure. We also note that the density of states at the Fermi level, $N(E_F)=1.6$ states/eV, is quite high and slightly larger than that of the 40 K superconducting MgB_2,[8] raising the question of possible superconductivity in ReB_2, which we will address later.

We next discuss the elastic constants of the relaxed ReB_2 structure, which was calculated directly. For hexagonal crystal, there are five independent elastic coefficients c_{11}, c_{12}, c_{13}, c_{33}, and c_{44}. Therefore, we applied five symmetry-independent strains[16] $(\gamma,\gamma,0,0,0,0)$, $(\gamma,-\gamma,0,0,0,0)$, $(0,0,\gamma,0,0,0)$, $(0,0,0,0,2\gamma,0)$, $(\gamma,\gamma,\gamma,0,0,0)$ to extract the five unknowns. We used γ of ±0.005, ±0.0075, ±0.01, ±0.015. From the least-square fit of the total energy vs strain data[17] (Fig. 3), we found that $c_{11}=641$ GPa, $c_{12}=159$ GPa, $c_{13}=128$ GPa, $c_{33}=1037$ GPa, and $c_{44}=271$ GPa. The quality of the data fit is excellent. By doubling the strain magnitudes, the fitted elastic constants only change slightly, suggesting that the anharmonicity is negligible in this structure. Note that our calculated elastic constant along the c axis $c_{33}=1037$ GPa is very large and indeed comparable to that of diamond (≈1040 GPa, the largest known elastic

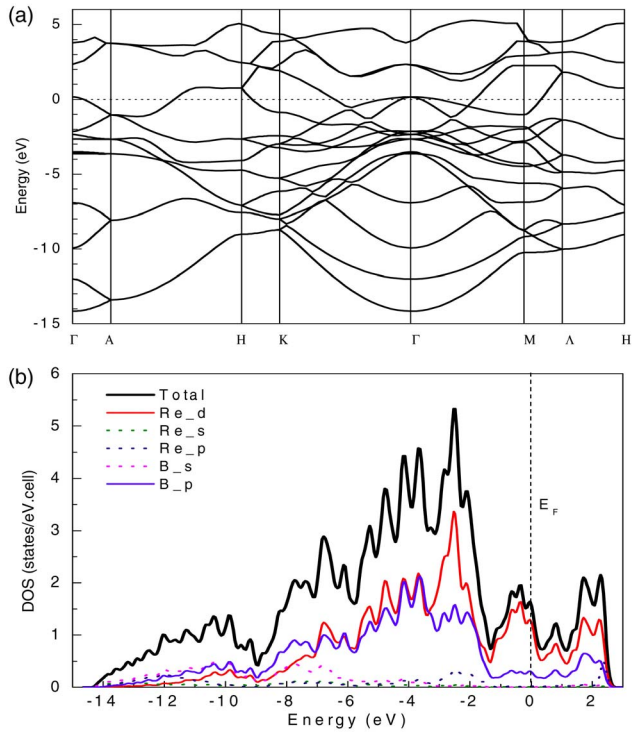

FIG. 2. (Color online) (a) The calculated electronic band structure of ReB_2, along high-symmetry directions in the Brillouin zone. Γ, *A*, *H*, *K*, *M*, and Λ represent *k* points (0 0 0), (0 0 0.5), (−1/3,2/3,0.5), (−1/3,2/3,0), (0, 0.5, 0), and (0, 0.5, 0.5), respectively. (b) The total and partial density of states (DOS) of ReB_2. The main feature of the electronic structure of ReB_2 is a strong hybridization of Re-*d* and B-*p* orbitals, which results in the strong covalent Re-B bond.

coefficient[18]). This result conforms well with the reported experimental observation, namely, that the incompressibility along the *c* axis is equal in magnitude to the linear incompressibility of diamond.[2] Also note the anisotropy in the compressibility of the two different lattice directions, i.e., the *a* axis is substantially more compressible than the *c* axis, which is also consistent with experimental observation. For a hexagonal crystal, the Voigt bulk modulus $B=2(c_{11}+c_{12}+2c_{13}+c_{33}/2)/9$, thus we obtain $B=350$ GPa, in good agreement with the experimental value[2] of ≈360 GPa. The Voigt shear modulus $G=(7c_{11}-5c_{12}-4c_{13}+2c_{33}+12c_{44})/9$, from which we obtain $G=283$ GPa. Comparing our calculated elastic coefficients with the computational results of Hao *et al.*,[3] we found only a small difference (<5%), which is likely due to the slight difference between different plane wave DFT codes.

Materials with high bulk and shear modulus are often hard materials. The hardness of a covalent or ionic compound can be directly calculated using the method recently proposed by Šimunek and Vackár,[19] based on analyzing bond strengths and their densities. As discussed earlier, in the ReB_2 crystals, each Re atom forms eight bonds with B atoms, six of which have $d_{\text{Re-B}}=2.257$ Å (bonding) while other two have slightly shorter $d_{\text{Re-B}}=2.227$ Å (antibonding). In addition, each B atom forms three covalent bonds with its neighboring B atoms ($d_{\text{B-B}}=1.820$ Å). The Re-Re interaction has a weak metallic nature with a nearest neighbor distance of 2.90 Å, thus their contribution to the hardness is negligible. The reference energies[19] (number of valence electron divided by the radius which makes the atom neutral) for Re and B were calculated to be 4.878 and 3.09, respectively. Using Eq. (6) in Ref. 19, we derived $H=46.0$ GPa. Although the anisotropy of the hardness was not considered here, the calculated average value falls right within the range of the experimentally measured hardness (≈30 to 56 GPa).[2]

Next, we discuss the phonon structure of ReB_2, which also reflects the mechanical properties. In addition, the lattice dynamics determine a wide range of other macroscopic behaviors such as thermal and transport properties, and the interaction with radiation (e.g., infrared absorption, Raman scattering, or inelastic neutron scattering). We performed the dynamical calculations on the optimized ReB_2 structure using the supercell method with finite difference.[20] A $2\times2\times1$ supercell was used, and the full dynamical matrix was obtained from a total of eight symmetry-independent atomic displacements (0.02 Å). The unit cell of ReB_2 contains six atoms, which give rise to a total of 18 phonon branches. The phonon modes at Γ are classified as

$$\Gamma(q=0)=A_{1g}+2A_{2u}(IR)+2B_{1g}+B_{2u}+E_{2u}+2E_{2g}(R)+2E_{1u}(IR)+E_{1g}(R),$$

where *R* and IR correspond to Raman and infrared active, respectively. The crystal symmetry implies six Raman- and six IR-active modes. In Table II, we list the calculated energies at Γ and corresponding mode characters.

The computed phonon dispersion curves and phonon density of states are shown in Fig. 4(a). The acoustic branches have steep slopes, indicating large elastic coefficients. Using the low-energy part of the acoustic branches (i.e., "elastic limit"), we can estimate the sound velocity (*V*) and thus also elastic constants. For example, for a hexagonal crystal, $c_{33}=\rho V(\text{longitudinal }[0001])^2$ and $c_{44}=\rho V(\text{transverse }[0001])^2$, where ρ is the mass density. We derived $c_{33}=948$ GPa and $c_{44}=278$ GPa. The slope determination close to $q=0$ certainly has some error bar; nevertheless, the above estimated values are still in reasonable agreement with the more precise numbers calculated earlier by directly applying strains.

The optical phonon branches are clearly divided into two groups. The three lowest energy optical modes (<30 meV) are dominated by Re motion while the high energy optical modes (>50 meV) are dominated by the lighter B atom displacement. Note that for similar types of atom motion, we found that those along *c* axis always have higher energies than the one within the basal *a*-*b* plane. This is due to the covalent Re-B bonding along the *c* axis. For boron motion within the plane, those involving B-B bond stretching (i.e., the motion of the bonded B-B pair being out-of-phase) are of higher energy than the in-phase motion, due to the strong B-B covalent bonding. Hence, the phonon structure is totally consistent with our ealier electronic structure analysis.

The calculated phonon structure is further validated by the neutron spectroscopy measurement. The measured INS spectrum is essentially the phonon DOS weighted by the neutron

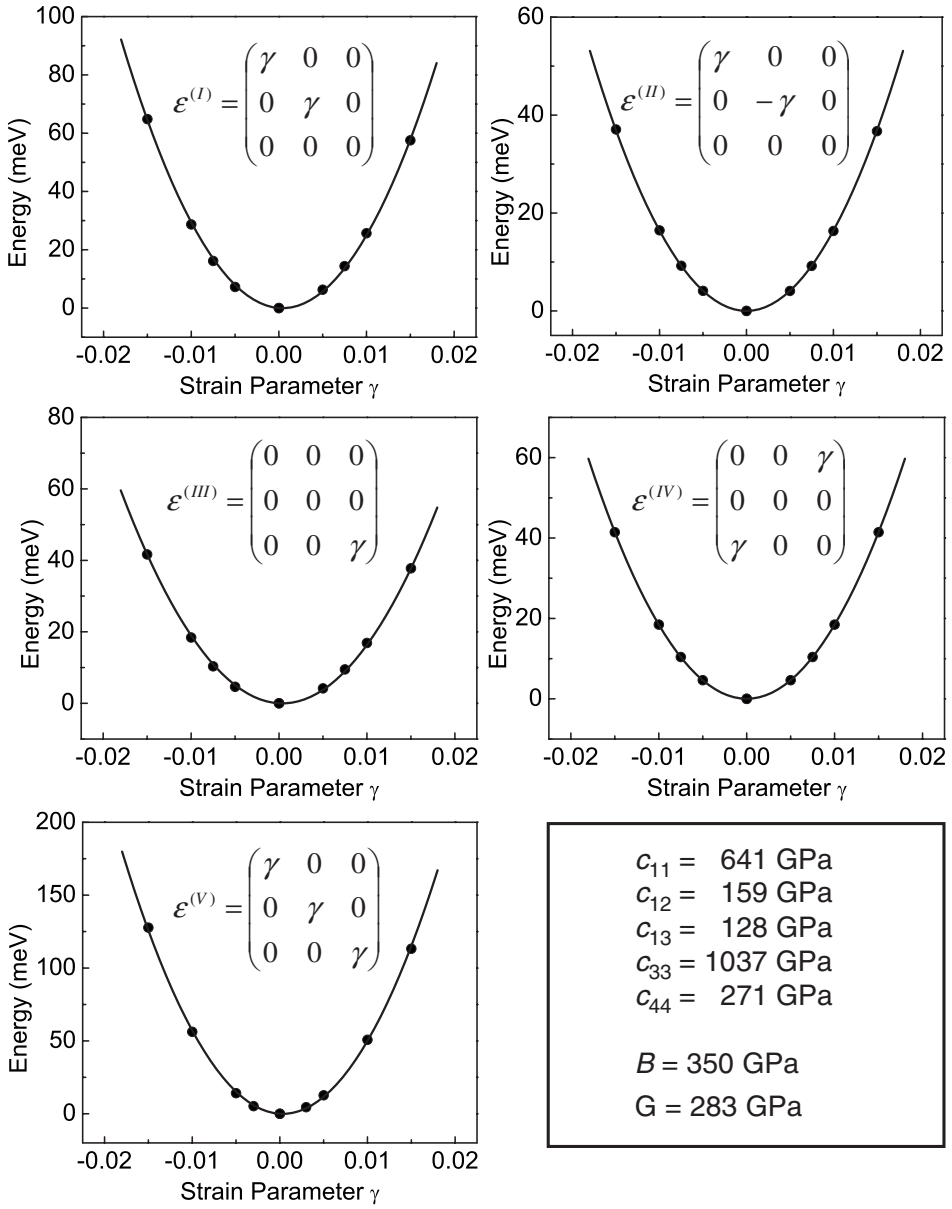

FIG. 3. Least-square fit of the total energy data vs strain parameters. The dots are from the first-principles calculations and the solid lines are the least-square fit. The deformation matrices for each distortion are also shown. The five hexagonal elastic constants of ReB_2, along with the bulk modulus and shear modulus are summarized in the right-bottom panel.

scattering cross sections of the elements. As shown in Fig. 4(b), the agreement between the experimental data and the calculated spectrum based on the incoherent approximation[21] is excellent.

It is interesting to note that the phonon structure of ReB_2 is quite similar to that of MgB_2, a high-T_c material.[8] With a MgB_2-like phonon spectrum and a slightly higher $N(E_F)$ than that of MgB_2 as mentioned earlier, one may wonder if ReB_2 can exhibit superconductivity at a "high" temperature. Experimentally, in the Re-B system, Re_3B and Re_7B_3 were found to have a T_c of 4.8 and 3.3 K, respectively.[22] We are not aware of any experimental measurement of T_c in ReB_2. We thus calculated the electron-phonon coupling parameters at Γ for ReB_2 and tried to estimate T_c. The results are shown in Table II. The coupling mainly takes place for B phonons along c axis. Compared to MgB_2, the electron-phonon coupling in ReB_2 is much weaker. Using the McMillian expression[23] and only considering the zone center phonon, T_c of ReB_2 is estimated to be less than 1 K. It would be interesting to confirm this estimate experimentally.

Finally, we discuss the thermal expansion of the ReB_2 structure, a property important for practical applications. The temperature dependence of the lattice parameters a and c are calculated within the quasiharmonic approximation. The results were obtained by minimizing the Helmholtz free energy

$$F(a,c,T) = V(a,c) + \sum_j \sum_{\mathbf{q}} \left\{ \frac{1}{2}\hbar\omega_j(\mathbf{q}) + kT\, ln(1 - e^{-\hbar\omega_j(\mathbf{q})/kT}) \right\},$$

where the first term is the ground-state energy and the second term is obtained by summing the phonon modes over the wavevectors in the Brillouin zone. In the quasiharmonic approximation, the effect of the anharmonicity in the lattice

TABLE II. The calculated phonon energies E and the characteristics of the optical modes of ReB_2 at Γ point. Note that in the table, "in-phase" and "out-of-phase" refer to the movement of the bonded B-B pair in the unit cell. (IR) and (R) indicates the IR and Raman active modes, respectively. The last column indicates the electron-phonon coupling for each modes at the Γ point, which are quite small compared to those of MgB_2.

Species	E (meV)	Dominant character/type	$\lambda_{el\text{-}ph}$
$2E_{2g}$	18.6	Re in a-b plane	0
B_{1g}	28.5	Re along c	0.007
$2E_{2u}$	50.1	B in a-b plane, in-phase	0
$2E_{1u}$	59.6	B in a-b plane, in-phase (IR)	0.008
A_{2u}	78.1	B along c, in-phase (IR)	0
$2E_{1g}$	85.2	B in a-b plane, out-of-phase (R)	0.002
B_{2u}	87.6	B along c, out-of-phase	0.025
$2E_{2g}$	90.4	B in a-b plane, out-of-phase (R)	0.016
B_{1g}	91.1	B along c, out-of-phase	0.021
A_{1g}	97.7	B along c, out-of-phase	0.018

energy is treated by allowing the phonon frequencies to depend on the lattice parameters. Hence, for a given temperature T, we first take a and c, minimize the atomic positions, and then calculate the phonon spectrum and the free energy. Repeating this for other values of a and c, we find the optimum values of the lattice parameters that minimize the free energy at a given temperature. In this way, one obtains the temperature dependence of a and c.

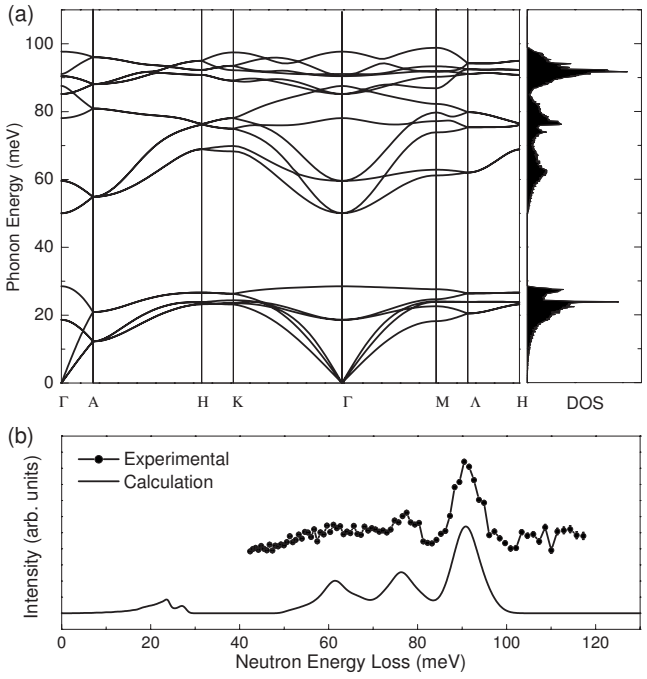

FIG. 4. (a) Calculated phonon dispersion curves along high-symmetry directions in the Brillouin zone for ReB_2 and the phonon density of states. (b) Inelastic neutron scattering spectrum from ReB_2 (at 4 K) along with the calculated spectrum. The agreement is excellent.

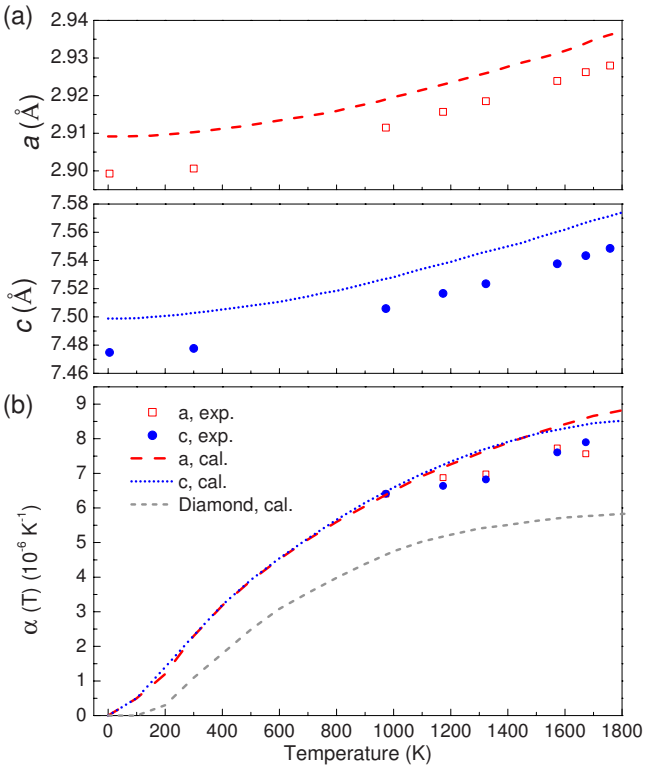

FIG. 5. (Color online) (a) The calculated (lines) and experimental (dots) temperature dependence of the structural parameters a and c of ReB_2. (b) The calculated (lines) and experimental (dots) linear thermal expansion coefficient of ReB_2. For comparison purpose, the calculated linear thermal expansion coefficient of diamond is also shown. The thermal expansion of ReB_2 is nearly isotropic and the magnitude is in the same order as that of diamond.

The calculated temperature dependence is shown in Fig. 5(a), along with the experimental lattice constants measured by neutron powder diffraction. Although the DFT-GGA calculation predicts slightly larger lattice constants than the measured values, the overall agreement on the lattice expansion is reasonably good. We found that the linear thermal expansion coefficients along a and c axes are both very small [see Fig. 5(b)], $\approx 6.5\times10^{-6}$ K^{-1} at 1000 K, slightly larger than that of diamond ($\approx 4.5\times10^{-6}$ K^{-1} at 1000 K). Additionally, a and c expansion coefficient curves nearly overlap with each other, suggesting that the material is highly isotropic in terms of thermal expansion, which is preferred in most applications. The excellent combination of hardness, incompressibility and small thermal expansion coefficient indicates that ReB_2 has great potential for many applications, such as material for cutting tools and abrasion resistance coating.

IV. CONCLUSIONS

In summary, we have applied density-functional theory and neutron scattering techniques to elucidate the electronic, elastic, phonon, and thermal properties of ReB_2. Our calculated elastic constants, bulk modulus, and hardness are in very good agreement with the experimental data. Our electronic and phonon results confirmed that the strong covalent

B-B bonding and Re-B bonding play a critical role in the incompressibility and hardness of ReB_2. Our calculations indicate that ReB_2 has a very similar phonon spectrum to MgB_2 with a comparable $N(E_F)$. However, we found a very small electron-phonon coupling, which suggests a very modest superconducting temperature. The thermal expansion coefficient is found only slightly larger than that of diamond. The combined excellent mechanical and thermal properties suggest great potential for ReB_2 to be used as a cutting or coating material. The excellent agreement found between DFT calculations and experimental measurements indicate that first-principles calculations are able to capture the main interactions in this class of superhard materials, and thus can be used to search, predict, and design other materials with properties (hardness, etc.) better than diamond.

ACKNOWLEDGMENT

The authors thank T. J. Udovic for technical help in the INS data collection.

*wzhou@nist.gov

[1] R. B. Kaner, J. J. Gilman, and S. H. Tolbert, Science **308**, 1268 (2005).
[2] H.-Y. Chung, M. B. Weinberger, J. B. Levine, A. Kavner, J.-M. Yang, S. H. Tolbert, and R. B. Kaner, Science **316**, 436 (2007).
[3] X. Hao, Y. Xu, Z. Wu, D. Zhou, X. Liu, X. Cao, and J. Meng, Phys. Rev. B **74**, 224112 (2006).
[4] S. Baroni, A. Dal Corso, S. de Gironcoli, P. Giannozzi, C. Cavazzoni, G. Ballabio, S. Scandolo, G. Chiarotti, P. Focher, A. Pasquarello, K. Laasonen, A. Trave, R. Car, N. Marzari, and A. Kokalj, http://www.pwscf.org/
[5] Regular boron contains ≈20% ^{10}B and ≈80% ^{11}B. The ^{10}B isotope has a very large neutron absorption cross section.
[6] S. La Placa and B. Post, Acta Crystallogr. **15**, 97 (1962).
[7] J. Nagamatsu, N. Nakagawa, T. Muranaka, Y. Zenitani, and J. Akimitsu, Nature (London) **410**, 63 (2001).
[8] T. Yildirim, O. Gülseren, J. W. Lynn, C. M. Brown, T. J. Udovic, Q. Huang, N. Rogado, K. A. Regan, M. A. Hayward, J. S. Slusky, T. He, M. K. Haas, P. Khalifah, K. Inumaru, and R. J. Cava, Phys. Rev. Lett. **87**, 037001 (2001).
[9] R. W. Cumberland, M. B. Weinberger, J. J. Gilman, S. M. Clark, S. H. Tolbert, and R. B. Kaner, J. Am. Chem. Soc. **127**, 7264 (2005).
[10] A. Savin, R. Nesper, S. Wengert, and T. F. Fässler, Angew. Chem., Int. Ed. Engl. **36**, 1808 (1997).
[11] M. D. Segall, R. Shah, C. J. Pickard, and M. C. Payne, Phys. Rev. B **54**, 16317 (1996).
[12] Z. Y. Chen, H. J. Xiang, J. Yang, J. G. Hou, and Q. Zhu, Phys. Rev. B **74**, 012102 (2006).
[13] M. Hebbache, L. Stuparevic, and D. Zivkovic, Solid State Commun. **139**, 227 (2006).
[14] S. Chiodo, H. J. Gotsis, N. Russo, and E. Sicilia, Chem. Phys. Lett. **425**, 311 (2006).
[15] H. Gou, L. Hou, J. Zhang, H. Li, G. Sun, and F. Gao, Appl. Phys. Lett. **88**, 221904 (2006).
[16] L. Fast, J. M. Wills, B. Johansson, and O. Eriksson, Phys. Rev. B **51**, 17431 (1995).
[17] Y. Le Page and Pa. Saxe, Phys. Rev. B **63**, 174103 (2001).
[18] G. Grimvall, *Thermophysical Properties of Materials* (North-Holland, Amsterdam, 1986).
[19] A. Šimunek and J. Vackár, Phys. Rev. Lett. **96**, 085501 (2006).
[20] T. Yildirim, Chem. Phys. **261**, 205 (2000).
[21] G. L. Squires, *Introduction to the Theory of Thermal Neutron Scattering* (Dover, New York, 1996).
[22] A. Kawano, Y. Mizuta, H. Takagiwa, T. Muranaka, and J. Akimitsu, J. Phys. Soc. Jpn. **72**, 1724 (2003).
[23] W. L. McMillan, Phys. Rev. **167**, 331 (1968).